Rank-one Detector for Kronecker-Structured Constant Modulus Constellations

Fazal-E-Asim, André L. F. de Almeida, Martin Haardt, Charles C. Cavalcante, and Josef A. Nossek

Abstract—To achieve reliable communication is indispensable for the high quality of service required by 5G. We propose a novel decoding strategy for constant modulus signals which is useful to provide low bit error ratios (BERs) in the low energy per bit to noise power spectral density ratio (Eb/No) regime with efficient computational complexity. The proposed strategy enjoys the benefit of exploiting the transmission of symbols as Kronecker products at the transmitter side. The proposed Kronecker-RoD (rank-one detector) is compared with convolutional codes with hard and soft Viterbi decoding. We observe that the Kronecker-RoD outperforms the latter in BER performance and has an efficient implementation complexity.

Index Terms—Kronecker coding, Convolutional encoding, Viterbi decoding, rank-one approximation, Least squares Kronecker factorization

I. INTRODUCTION

The next generation of cellular communication system promises high data rates, coverage, and responsiveness of communication networks [1]. Channel coding becomes an important player to reduce the errors introduced by a random channel. Low-density parity-check (LDPC), Turbo and convolutional codes are major candidates [2].

In [3], the authors proposed a multidimensional signal constellation design based on Euclidean space, which is used for spherical and non-spherical codes. In [4], a gradient search algorithm is used to optimize the rotation angle for M-PSK/M-QAM schemes which improves the performance as compared to the traditional schemes. Furthermore, the impact of coding/modulation for fading channels is discussed in [5].

In [6], a new parallel, symbol detection technique for M-PSK is proposed to speed up the detection process as compared to the conventional suboptimal detectors.

The least squares Kronecker factorization is proposed as a signal processing tool in [7] while a discussion about the extension of the Kronecker factorization to multiple Kronecker products is explained in [8], [9]. This paper has the following major contributions.

- We introduce a novel method of representing M-PSK constellations as Kronecker products of smaller constellations, referred to as Kronecker coding.
- To exploit the benefit of Kronecker coding at the receiver side, an efficient detection strategy is proposed that is

based on a rank-one approximation of the received data tensor. The proposed Kronecker-RoD (rank-one detector) is conceptually simple, operates with short data blocks, and has a smaller implementation complexity than state-of-the-art detectors.

- As shown in our numerical results, the Kronecker-RoD has a superior BER (bit error ratio) performance than hard and soft Viterbi decoding at the same spectral efficiency.

Notation: Scalars are denoted by lower-case italic letters $(a, b, \dots)$, vectors by bold lower-case italic letters $(\boldsymbol{a}, \boldsymbol{b}, \dots)$, matrices by bold upper-case italic letters $(\boldsymbol{A}, \boldsymbol{B}, \dots)$, tensors are defined by calligraphic upper-case letters $(\mathcal{A}, \mathcal{B}, \dots)$, $\boldsymbol{A}^{\mathrm{T}}, \boldsymbol{A}^{*}, \boldsymbol{A}^{\mathrm{H}}$ stand for transpose, conjugate and Hermitian of $\boldsymbol{A}$, respectively. The operators $\otimes$ and $\circ$ define the Kronecker and the outer product, respectively. The frontal slices of a third-order tensor $\mathcal{Y} \in \mathbb{C}^{L_1 \times L_2 \times L_3}$ are matrices denoted by $[\mathcal{Y}]_{..l_3} \in \mathbb{C}^{L_1 \times L_2}$, with $l_3 = \{1, \dots, L_3\}$. For an Nth order tensor $\mathcal{Y} \in \mathbb{C}^{L_1 \times \dots \times L_N}$, there are several ways to matricize it. The n-mode unfolding of $\mathcal{Y}$ is the matrix defined as $[\mathcal{Y}]_{(n)} = \mathbb{C}^{L_n \times L_1, \dots, L_{n-1} L_{n+1}, \dots L_N}$. The generalized unfolding is the matrix where the rows and columns are defined by grouping a subset of dimensions.

II. SYSTEM MODEL

We consider a single-input-single-output (SISO) wireless communication system. The received vector $\boldsymbol{y}[k] \in \mathbb{C}^{L \times 1}$ is represented as

$$\boldsymbol{y}[k] = h[k]\boldsymbol{x}[k] + \boldsymbol{n}[k] \qquad (1)$$

where $\boldsymbol{x}[k] \in \mathbb{C}^{L \times 1}$ is the transmitted data drawn from a constant modulus constellation, $h[k]$ represents the complex fading channel, L is the length of the data block, and $\boldsymbol{n}[k] \in \mathbb{C}^{L \times 1}$ is the additive white Gaussian noise according to $\boldsymbol{n}[k] \sim \mathcal{CN}(\boldsymbol{0}_{L \times 1}, \sigma_n^2 \mathbf{I}_L)$ where σ_n^2 is the variance of the noise. We propose a Kronecker-structured constellation design for the transmitted data according to

$$\boldsymbol{x}[k] = \boldsymbol{s}_N[k] \otimes \dots \otimes \boldsymbol{s}_1[k] \qquad (2)$$

where $\boldsymbol{s}_n[k] \in \mathbb{C}^{L_n \times 1}$, $n = \{1, \dots, N\}$, and

$$L = \Pi_{n=1}^{N} L_n \qquad (3)$$

The system model is shown Fig. 1. The vector $\boldsymbol{s}_n[k], n = \{1, \dots, N\}$ contains constant modulus symbols. At the transmitter, the serial data is converted to N-parallel data streams. At the n-th branch, the binary data is modulated to form symbol vectors $\boldsymbol{s}_n[k], n = \{1, \dots, N\}$. After modulation, Kronecker coding is applied, and the resulting symbol stream is transmitted. At the receiver the Kronecker-RoD is applied,

Fazal-E-Asim, André L. F. de Almeida, Charles C. Cavalcante and Josef A. Nossek are with the Department of Teleinformatics Engineering, Federal University of Ceará, Fortaleza, Brazil. Josef A. Nossek is also with the Department of Electrical and Computer Engineering, Technical University of Munich, Germany. Martin Haardt is with the Communications Research Laboratory, Ilmenau University of Technology, Ilmenau, Germany. e-mail: {fazalasim, josef.a.nossek, charles, andre}@gtel.ufc.br, martin.haardt@tu-ilmenau.de
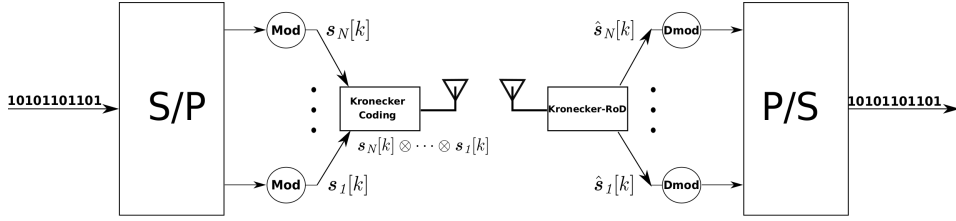
Fig. 1. Kronecker coding and decoding.

as explained in Section III, to estimate the symbol vectors $\hat{s}_n[k], n = \{n = 1, \ldots, N\}$, which are demodulated and converted back to a serial data stream.

III. KRONECKER-RANK-ONE DETECTOR (KRONECKER-RoD)

A. Kronecker Factorization of M-PSK Constellation

To exploit the benefit of Kronecker structured constellations at the receiver, it is important to understand the principles behind the transmission of Kronecker products of a constellation. The key principle is that any M-PSK constellation can be expressed as the Kronecker product of two or more constant modulus constellations of equal or smaller cardinalities. For illustration purposes, let us consider the case shown in Fig. 2. A 16-PSK constellation is shown in Fig. 2(a). Note that any point in this constellation is the result of the Kronecker product of the three smaller contant modulus constellations shown in Fig.s 2(b),2(c), and 2(d), respectively.

(a) $s = s_1 \otimes s_2 \otimes s_3 \in$ 16-PSK   (b) s_1
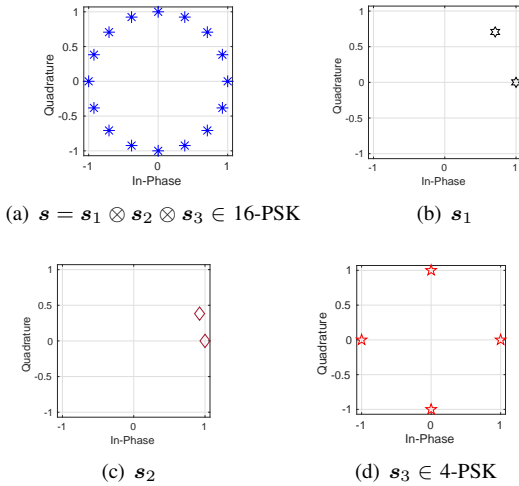
(c) s_2 (d) $s_3 \in$ 4-PSK

Fig. 2. Kronecker coding of more than two small constellations.

Fig. 3 shows the other side of the story, where two 4-PSK signals result in another 4-PSK constellation. The same is valid for higher cardinalities and multiple Kronecker products involving $s_1[k], \ldots, s_N[k]$. In the following, we exploit this concept to derive a new coding and decoding scheme that exploits the Kronecker structure of our designed constant modulus constellation. The proposed scheme is an attractive solution for short data blocks.

The code rate for the Kronecker coding is given by

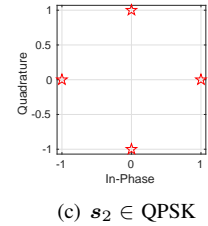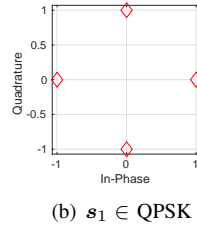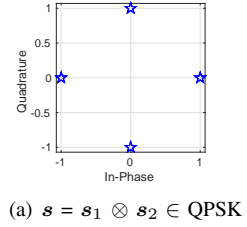$$R = \frac{\sum_{n=1}^{N} L_n}{\Pi_{n=1}^{N} L_n}. \tag{4}$$

(a) $s = s_1 \otimes s_2 \in$ QPSK

(b) $s_1 \in$ QPSK   (c) $s_2 \in$ QPSK

Fig. 3. Kronecker coding of two known constellations.

where R represents the code rate, L_n is the length of the symbol vector s_n, and N represents the number of symbol vectors involved in the Kronecker coding operation, to generate the transmitted signal shown in (2).

B. Tensor Power Method Detector

The received signal after matched filtering is given by

$$\hat{y}[k] = h^*[k]y[k]. \tag{5}$$

For notational convenience, we skip the index $[k]$ in the rest of this paper. From (1) and (2), the estimation of the transmitted data x can be translated into the solving the following problem

$$\min_{s_N, \ldots, s_1} \left\| \hat{y} - s_N \otimes \cdots \otimes s_1 \right\|_2^2. \tag{6}$$

Note that (2) can be recast as a rank-one tensor $\mathcal{X} = s_1 \circ \cdots \circ s_N \in \mathbb{C}^{L_1 \times L_2 \cdots \times L_N}$. Hence, problem (6) can be rewritten as

$$\min_{s_1, \ldots, s_N} \left\| \hat{\mathcal{Y}} - s_1 \circ \cdots \circ s_N \right\|_F^2, \tag{7}$$

where $\mathcal{Y} \in \mathbb{C}^{L_1 \times L_2 \cdots \times L_N}$ is the N-th order received data tensor. Indeed, since $\mathcal{Y}$ is a scaled version of $\mathcal{X}$ corrupted by additive Gaussian noise, estimating the transmitted symbols $s_1, \ldots, s_N$ translates into finding a rank-one approximation to $\mathcal{Y}$. It is well known that a solution to this problem is provided by the truncated higher-order singular value decomposition (HOSVD) [10], [11]. An efficient way to compute

this truncated rank-one HOSVD is the tensor power method [12]–[14]. As shown in [14], minimizing the cost function in (7) is equivalent to maximizing the following tensor Rayleigh quotient

$$\max_{\boldsymbol{s}_N,\ldots,\boldsymbol{s}_1} \frac{\left|(\boldsymbol{s}_N \otimes \cdots \otimes \boldsymbol{s}_1)^{\mathrm{T}} \mathrm{vec}(\hat{\mathcal{Y}})\right|}{\|\boldsymbol{s}_1\|_2 \ldots \|\boldsymbol{s}_N\|_2} \tag{8}$$

We propose a tensor power method detector (TPMD), where an estimate $\hat{\boldsymbol{s}}_n, n = \{1,\ldots,N\}$ is found from the dominant left singular vectors $\boldsymbol{u}_n \in \mathbb{C}^{L_n \times 1}$ (up to scaling) of the n-mode unfolding $[\mathcal{Y}]_{(n)}$ of the received data tensor $\mathcal{Y}, \{n = 1,\ldots,N\}$.

For simplicity, let us define the following Gramian

$$\boldsymbol{A}_n = [\mathcal{Y}]_{(n)}[\mathcal{Y}]_{(n)}^{\mathrm{H}} \in \mathbb{C}^{L_n \times L_n} \tag{9}$$

where $n = 1,\ldots,N$. The TPMD starts from the initializations $\boldsymbol{u}_1^0,\ldots,\boldsymbol{u}_N^0$ of the N symbol vectors, which are randomly drawn from their respective known $M-$PSK alphabets. At the $j-$th iteration, a new estimate is found by $\boldsymbol{u}_n^{(j)} = \boldsymbol{A}_n\boldsymbol{u}_n^{(j-1)}$. Due to the unknown norm of $\boldsymbol{u}_n$, we have $\hat{\boldsymbol{s}}_n = \beta_n\boldsymbol{s}_n, n =$

Algorithm 1 Tensor Power Method Detector

1: **procedure** TPMD($\mathcal{Y}$)
2:     $\mathcal{Y} \leftarrow \hat{\boldsymbol{y}}$
3:     **for** $n = 1 : N$ **do**
4:        Initialize $\boldsymbol{u}_n^{(0)}$ with random M-PSK symbols
5:        **for** $j = 1 : J$ **do**
6:           $\boldsymbol{u}_n^{(j)} = \boldsymbol{A}_n\boldsymbol{u}_n^{(j-1)}$
7:        **end for** J **iterations.**
8:        $\beta_n = \frac{\boldsymbol{u}_n[1]}{\boldsymbol{s}_n[1]}$
9:        $\hat{\boldsymbol{s}}_n = \frac{\boldsymbol{u}_n}{\beta_n}$
10:        **return** $\hat{\boldsymbol{s}}_n$
11:     **end for** N**-modes of** $\mathcal{Y}$
12: **end procedure**

$\{n = 1,\ldots,N\}$, where β_n is a scaling factor. In order to estimate such a scaling ambiguity, we propose setting one symbol of $\boldsymbol{s}_n, n = \{n = 1,\ldots,N\}$, as a pilot symbol known to the receiver. In this case, the scaling factor β_n can be determined as

$$\beta_n = \frac{\boldsymbol{u}_n[1]}{\boldsymbol{s}_n[1]}, \tag{10}$$

where $\boldsymbol{u}_n[1]$ is first element of $\boldsymbol{u}_n$ and $\boldsymbol{s}_n[1]$ is the known pilot symbol in $\boldsymbol{s}_n$. The n-th estimated symbol vector is then obtained as

$$\hat{\boldsymbol{s}}_n = \frac{\boldsymbol{u}_n}{\beta_n}. \tag{11}$$

Since the estimation of $\hat{\boldsymbol{s}}_1,\ldots,\hat{\boldsymbol{s}}_N$ can be carried out independently, the N branches of the Kronecker-RoD shown in Fig. 4 can be executed in parallel. The TPMD algorithm is summarized in Algorithm 1.

C. Computational Complexity Analysis

In this section, the complexity of the overall Kronecker-RoD method is discussed. In the Kronecker-RoD method, the TPMD algorithm is used for every unfolding of the tensor $\mathcal{Y}$,
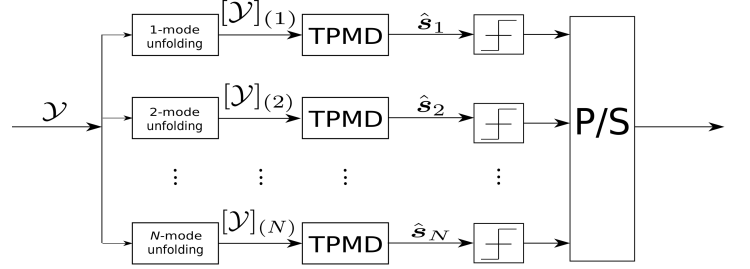

Fig. 4. Implementation of Kronecker-RoD as parallel TMPD branches.

so the complexity of the Kronecker-RoD actually boils down to N times the computational complexity of TPMD. In general, we consider the complexity of the product of two complex matrices as $4MNR$ multiplications given $\mathbf{A} \in \mathbb{C}^{M \times R}$ and $\mathbf{B} \in \mathbb{C}^{R \times N}$ [14].

To find the complexity of TPMD, let us use the example of the unfolding of a fourth order tensor formed by the Kronecker products of vectors having equal length $\boldsymbol{s}_n \in \mathbb{C}^{L_n \times 1}$, $[\mathcal{Y}]_{(n)} = L_n \times L_n^3$. Therefore the computationally complexity of line (6) in Algorithm 1 is $O\left(8L_n^4\right)$. The total complexity for each each branch in Fig. 1 is $O(J(8L_n^4))$. Finally the overall complexity of the Kronecker-RoD is given as $O(N(J(8L_n^4)))$.

IV. NUMERICAL RESULTS

In this section, we evaluate the bit error ratio (BER) performance of the Kronecker-RoD in a single input single output (SISO) system using an i.i.d. Rayleigh channel. For each symbol vector $\boldsymbol{s}_1,\ldots,\boldsymbol{s}_N$, both 2-PSK and 4-PSK modulations are used. To provide good references for comparisons, we compare the performance of Kronecker-RoD with $N = 2, 3$ and 4 TPMD branches with that of a conventional convolutional encoding/decoding scheme, as well as hard and soft Viterbi decoders [15]. In this comparison we use M-PSK modulation schemes for all transmitted symbol vectors $\boldsymbol{x} = \boldsymbol{s}_N \otimes \cdots \otimes \boldsymbol{s}_1$ as mentioned in Fig. 3.

The convergence of the TPMD is analyzed considering the criteria that the minimum error approaches using the stopping threshold of 10^{-6}, which comes out that $J = 10$, iterations are needed to meet the stopping threshold. Furthermore, we have found that by reducing the number of iterations to $J = 3$, we obtain the same performance.

To ensure a fair comparison, a half-rate convolutional encoder is used. To keep the same data rate and spectral efficiency, for all the simulated schemes and experiments, we assume the transmission of $L = 8$ bits when considering 2-PSK modulation, and $L = 16$ bits for 4-PSK modulation.

Our first experiments consider an AWGN channel. In Fig. 5, we compare the performance of the different schemes for 2-PSK modulation, resulting in half-rate transmission for all of them. First, note that by increasing the number N of Kronecker-encoded symbol vectors (2), or equivalently, the number of parallel TPMD branches, (see Fig. 4), the BER performance is improved. For a target BER of 10^{-2}, TPMD-4 provides a Eb/No gain of approximately 2 dB over TPMD-2. Such an improvement comes from the enhanced noise rejection capability of Kronecker-RoD as N increases, due to the tensor
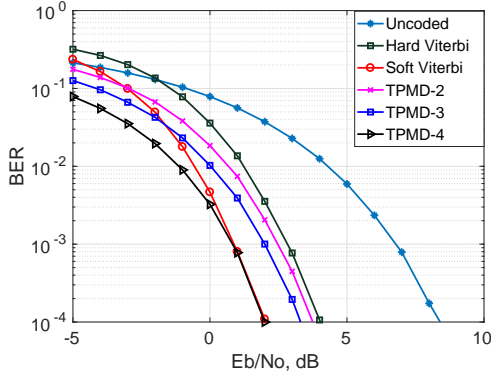
Fig. 5. BER performance of Kronecker-RoD with $N = 2$, 3 and 4 TPMD branches. As a reference for comparison, we plot the conventional convolutional encoding/decoding scheme, as well as hard and soft Viterbi decoders. In all cases, 2-PSK constellation is assumed.
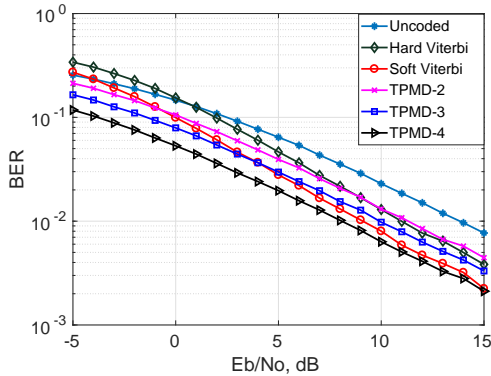

Fig. 7. BER performance of Kronecker-RoD with $N = 2$, 3 and 4 TPMD branches. As a reference for comparison, we plot the conventional convolutional encoding/decoding scheme, as well as hard and soft Viterbi decoders. In all cases, 4-PSK constellation is assumed.

Fig. 6. BER performance of Kronecker-RoD with $N = 2$, 3 and 4 TPMD branches under a flat-fading channel and 2-PSK modulation.

Fig. 8. BER performance of Kronecker-RoD with $N = 2$, 3 and 4 TPMD branches under a flat-fading channel and 4-PSK modulation.

gain. We can also observe that TPMD-4 outperforms the soft Viterbi decoder for the lower Eb/No range and significantly outperforms the hard Viterbi decoder. In Fig. 7, the same comparisons are drawn assuming 4-PSK modulation. Note that the BER gains of Kronecker-RoD over the competing schemes are higher in comparison with the 2-PSK case.

Next, the flat-fading channel is included in our simulation study (1). At each run, the channel coefficient is drawn from a zero mean unit variance complex Gaussian distribution. The results are shown in Fig.s 6 and 8, for 2-PSK and 4-PSK modulations, respectively. Note that Kronecker-RoD with TPMD-3 and TPMD-4 outperforms the hard decision Viterbi decoder for the whole Eb/No range. In particular, TPMD-4 provides lower error rates than soft Viterbi for lower Eb/No levels. The gains are even more pronounced when considering 4-PSK modulation in Fig. 8. For instance, considering a target BER of 10^{-2}, Kronecker-RoD with three branches (TPMD-3) provides an Eb/No gain of 2 dB over soft Viterbi. Using four branches (TPMD-4) offers a 4 dB gain in terms of Eb/No over soft Viterbi, which is a remarkable result.

Next, we compare the computational complexity which causes delay in the decoding process of the proposed Kronecker-RoD algorithm and Viterbi decoding. For the latter, we use the constraint length $K = 3$ with the generators in octal
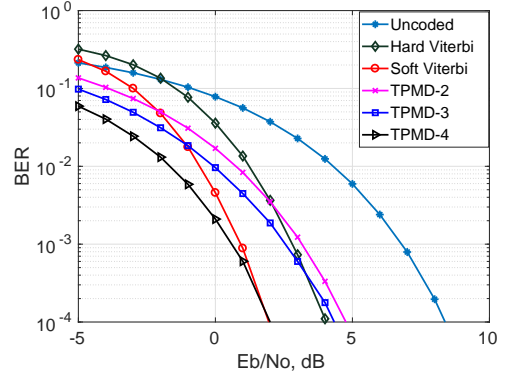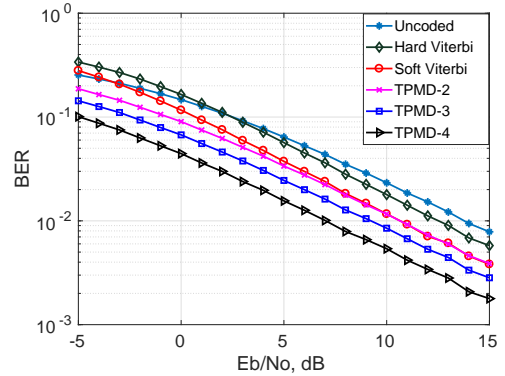
form as $(7, 5)$ which gives half-rate. The actual decoding delay of symbols into data can be found by tracing the maximum likelihood path backwards through the trellis. In practice, the decoder starts to decode bits once it has reached a time equal to five times the constraint length $5K = 5(3) = 15$, [15], [16], while in our proposed Kronecker-RoD case, the delay is dependent on the size of the block which is $L = 16$.

V. CONCLUSION

In this paper, we propose a novel encoding strategy at the transmitter using Kronecker products of M-PSK and a new decoding strategy using the Kronecker-RoD receiver. The Kronecker-RoD is applying TPMD on each unfolding of the received tensor which can be applied in parallel. The Kronecker-RoD outperforms the state-of-the-art schemes based on the BER metric with the same delay. The Kronecker-RoD can be further extended to multiple-input-multiple-output (MIMO) systems.

REFERENCES

[1] G. R. Patil and P. S.Wankhade, "5G wireless technology," *International Journal of Computer Science and Mobile Computing*, vol. 3, no. 2, pp. 203–207, October 2014.

[2] A. Goel and M. K. Garg, "Comparative performance evaluation of convolutionally coded and LDPC coded OFDM system over AWGN and SUI-5 fading channel," in *Proc. 2012 Third International Conference on Computer and Communication Technology*, Nov 2012, pp. 250–254.

[3] J. Porath and T. Aulin, "Design of multidimensional signal constellations," *IEE Proceedings - Communications*, vol. 150, no. 5, pp. 317–, Oct 2003.

[4] M. N. Khormuji, U. H. Rizvi, G. J. M. Janssen, and S. B. Slimane, "Rotation optimization for MPSK/MQAM signal constellations over Rayleigh fading channels," in *Proc. 2006 10th IEEE Singapore International Conference on Communication Systems*, Oct 2006, pp. 1–5.

[5] E. Biglieri, J. Proakis, and S. Shamai, "Fading channels: information-theoretic and communications aspects," *IEEE Transactions on Information Theory*, vol. 44, no. 6, pp. 2619–2692, Oct 1998.

[6] G. Hegde, Y. Yang, C. Steffens, and M. Pesavento, "Parallel low-complexity M-PSK detector for large-scale MIMO systems," in *proc. 2016 IEEE Sensor Array and Multichannel Signal Processing Workshop (SAM)*, July 2016, pp. 1–5.

[7] C. F. Van Loan and N. Pitsianis, "Approximation with Kronecker Products." in *Linear Algebra for Large Scale and Real-Time Applications, Springer*, vol. 232, 1992, pp. 293–314.

[8] King Keung Wu, Y. Yam, H. Meng, and M. Mesbahi, "Kronecker product approximation with multiple factor matrices via the tensor product algorithm," in *Proc. 2016 IEEE International Conference on Systems, Man, and Cybernetics (SMC)*, Oct 2016, pp. 004 277–004 282.

[9] B. Sokal, A. de Almeida, and M. Haardt, "Semi-blind receivers for MIMO multi-relaying systems via rank-one tensor approximations," *Signal Processing*, vol. 166, pp. 2619–2692, Jan 2020.

[10] L. De Lathauwer, B. De Moor, and J. Vandewalle, "A multilinear singular value decomposition," *SIAM Journal on Matrix Analysis and Applications*, vol. 21, no. 4, pp. 1253–1278, 2000.

[11] T. G. Kolda and B. W. Bader, "Tensor decompositions and applications," *SIAM Review*, vol. 51, no. 3, pp. 455–500, 2009.

[12] L. D. Lathauwer, P. Comon, B. D. Moor, and J. Vandewalle, "Higher-order power method - application in independent component analysis," in *Proc. NOLTA Conference, volume 1, pp. 91–96, Las Vegas,*, 1995.

[13] P. A. Regalia and E. Kofidis, "The higher-order power method revisited: convergence proofs and effective initialization," in *Proc. 2000 IEEE International Conference on Acoustics, Speech, and Signal Processing.*, vol. 5, June 2000, pp. 2709–2712 vol.5.

[14] G. H. Golub and C. F. Van Loan, "Matrix Computations." in *4th edition. Johns Hopkins University Press, Maryland, Baltimore, USA*, 2013.

[15] A. Viterbi, "Error bounds for convolutional codes and an asymptotically optimum decoding algorithm," *IEEE Transactions on Information Theory*, vol. 13, no. 2, pp. 260–269, April 1967.

[16] B. Moision, "A truncation depth rule of thumb for convolutional codes," in *Proc. 2008 Information Theory and Applications Workshop*, Jan 2008, pp. 555–557.